Technobius Physics, 2025, 3(4), 0041, DOI: https://doi.org/10.54355/tbusphys/3.4.2025.0041

Technobius Physics

https://technobiusphysics.kz/

e-ISSN 3007-0147

Review

Electron hydrodynamics in ultra-clean conductors: from Dirac fluids in graphene to viscous metals

David Paulsen*.

Faculty of Science and Engineering, Queen Mary University of London, London, United Kingdom
*Correspondence: paulsend27@gmail.com

Abstract. This work examines the emerging field of electron hydrodynamics in ultra-clean conductors, where charge carriers behave collectively as a viscous fluid rather than as independent quasiparticles. The objective is to provide a unified perspective that connects theoretical frameworks with key experimental realizations in graphene, delafossite metals and topological semimetals. To this end, we performed a structured literature search across major databases and preprint servers, applied explicit inclusion and exclusion criteria to identify genuinely hydrodynamic studies, and carried out a comparative, narrative analysis of transport, thermal and imaging experiments. The collected evidence shows that hydrodynamic transport arises when electron–electron collisions dominate over momentum-relaxing processes and when device dimensions are comparable to characteristic scattering lengths. In this regime, experiments reveal geometry-dependent resistivity, negative nonlocal signals, super-ballistic conductance, strong violations of the Wiedemann–Franz law and, in some cases, Hall viscosity. Graphene provides the clearest realization of a relativistic Dirac fluid, while $PdCoO_2$ and WP_2 demonstrate that viscous electron flow also occurs in anisotropic and multi-band metals. This work highlights that boundaries, disorder and Fermi-surface geometry critically shape hydrodynamic signatures and must be incorporated into any quantitative interpretation. It identifies open issues concerning the roles of phonons and Umklapp processes, the reliable extraction of viscosity, and the extension of hydrodynamics to more complex correlated and topological phases. Finally, it outlines priorities for future “benchmark” experiments that combine nonlocal transport, thermal measurements and real-space imaging within the same devices.

Keywords: electron hydrodynamics, viscous electron flow, Dirac fluid, graphene transport, ultra-clean conductors, delafossite metals.

1. Introduction

In recent years, the idea that electrons in solids can behave collectively as a viscous fluid has evolved from a theoretical curiosity into an experimentally established transport regime. When electron–electron collisions occur much more frequently than momentum-relaxing scattering from impurities and phonons, charge carriers may form a locally equilibrated “electron liquid” governed by hydrodynamic equations rather than by the familiar Drude–Boltzmann picture [1]. In this regime, electrical and thermal transport acquire a pronounced sensitivity to device geometry and boundary conditions, leading to phenomena such as Poiseuille flow, negative nonlocal resistance, strongly modified Lorenz ratios and, in magnetic fields, Hall viscosity. Beyond their conceptual appeal, these effects open a route to probing interaction-dominated transport in quantum materials and to engineering devices that exploit, rather than suppress, electron–electron scattering [2], [3].

A systematic framework for classifying and analysing such regimes has been developed in a series of theoretical works on two-dimensional electron systems and, in particular, on graphene [4], [5], [6]. Narozhny’s reviews [7], [8] emphasize that hydrodynamic transport appears in a well-defined window between ballistic and diffusive regimes, characterized by a clear hierarchy of scattering times and by length scales comparable to device dimensions. Within this window, electron liquids can

display relativistic Dirac-fluid behaviour, quantum-limited viscosity and Planckian dissipation [9], [10], [11]. Building on this foundation, more recent theory has extended hydrodynamics to anisotropic and multi-band materials, demonstrating that Fermi-surface geometry and crystalline anisotropy qualitatively reshape current streamlines and nonlocal responses. In parallel, a growing body of experiments on graphene, delafossite metals and topological semimetals has revealed concrete realizations of viscous electron flow and associated anomalies in nonlocal transport, thermal conductivity and imaging [12], [13], [14].

The rapid expansion of this literature motivates a critical and comparative review. Existing surveys focus either on the general theoretical formalism [8], [15], [16] or on specific material platforms, most notably graphene [17]. However, the field has now reached a stage where hydrodynamic signatures have been reported in conceptually distinct systems—relativistic Dirac fluids, quasi-two-dimensional layered oxides and topological semimetals—often using different experimental probes and analysis strategies [18], [19], [20]. Without a unified perspective, it is difficult to assess which observations reflect a common hydrodynamic mechanism, which depend sensitively on sample quality and device design, and where alternative interpretations (ballistic transport, inhomogeneous disorder, phonon-dominated heat flow) remain viable.

The main objective of this review is therefore threefold. First, we aim to synthesise the current theoretical understanding of electron hydrodynamics in ultra-clean conductors, with particular emphasis on the regime classification and observable signatures articulated in Refs. [6], [1], [2], [3]. Second, we critically examine key experimental platforms—graphene, $PdCoO_2$ and WP_2—highlighting how different probes (nonlocal transport, thermal measurements and real-space imaging) reveal complementary aspects of hydrodynamic behaviour [19], [20], [21], [22]. Third, by comparing parameter regimes, device geometries and data-analysis strategies across these systems, we identify common trends and outstanding discrepancies, and use them to delineate promising directions for future work. In doing so, our goal is not only to summarise the state of the art, but also to provide a coherent framework within which new experiments and theories on electronic hydrodynamics can be interpreted.

2. Methods

This review is based on a structured and expert-guided survey of the contemporary literature on electron hydrodynamics in ultra-clean conductors, with emphasis on graphene, layered oxides and topological semimetals. We combined systematic database searches with targeted citation chasing in order to capture both the early theoretical proposals and the most recent experimental realizations of viscous electron flow. Literature searches were performed in Web of Science, Scopus, INSPIRE-HEP, arXiv and Google Scholar over the period from approximately 2010 to June 2025. Search queries combined controlled keywords such as “electron hydrodynamics,” “viscous electron flow,” “Poiseuille flow,” “Hall viscosity,” “Dirac fluid,” “negative nonlocal resistance,” “super-ballistic transport,” and “Planckian dissipation,” with material-specific terms including “graphene,” “delafossite,” “$PdCoO_2$,” “WP_2,” “WTe_2,” and “topological semimetal.” The initial query set and vocabulary were informed by established theoretical and review articles on electronic hydrodynamics in graphene and related systems [1], [2], [3], [4].

From the raw search output we first performed a coarse screening based on titles and abstracts. We retained studies that addressed charge or heat transport in solid-state electronic systems, explicitly invoked a hydrodynamic or viscous-flow description of electrons (rather than purely ballistic or diffusive models), and reported either experimental signatures of hydrodynamic behavior or theoretical analyses directly linked to experimentally accessible observables. Experimental “anchor” works at this stage included reports of negative nonlocal resistance and viscous backflow in graphene [5], observation of the Dirac fluid and breakdown of the Wiedemann–Franz law near charge neutrality [6], direct visualization of Poiseuille-like flow in narrow graphene channels [8], evidence for hydrodynamic transport in the delafossite metal $PdCoO_2$ [21], and thermal and electrical signatures

of viscous electron flow in tungsten diphosphide [15]. We also included imaging experiments that revealed spatial current patterns inconsistent with Ohmic transport, such as parabolic profiles and current whirlpools, and that explicitly interpreted these observations in terms of a finite electronic viscosity [8], [10]. Papers in which the term “hydrodynamic” was used only metaphorically, or applied exclusively to phonons, magnons, or classical fluids without direct connection to electronic transport, were excluded at this stage.

Full-text screening then applied stricter inclusion criteria. For an experimental study to be classified as genuinely hydrodynamic, we required that it provided evidence for a hierarchy of scattering times consistent with the hydrodynamic window,

$$\tau_{ee} \ll \tau_{imp}, \tau_{ph} \tag{1}$$

Where, τ_{ee} — electron–electron scattering time; τ_{imp} — impurity scattering time; τ_{ph} — phonon scattering time. As discussed in standard theoretical treatments [1], [2], [3], and that it identified non-trivial dependencies of transport coefficients on sample geometry or boundary conditions, for example, width-dependent resistivity, super-ballistic conductance through constrictions, or Poiseuille-type current profiles [5], [7], [8], [10], [11]. Alternatively, we accepted thermoelectric and thermal measurements that showed a strong decoupling of charge and heat currents—typically manifested as pronounced violations of the Wiedemann–Franz law or anomalous Lorenz ratios—interpreted within a hydrodynamic framework [6], [9]. In addition, we required sufficient detail about sample quality (mobility, residual resistivity, disorder characterization), device geometry and measurement configuration to allow a meaningful assessment of the realized transport regime. When classification was ambiguous, the work was retained but flagged for critical discussion in the Results and Discussion sections.

On the theoretical side, we focused on contributions that built a hydrodynamic or kinetic-theory description of electronic transport in realistic condensed-matter systems and that could be confronted with experiment. This included derivations of Navier–Stokes-type equations for electron liquids with specific band structures and disorder landscapes, calculations of transport coefficients such as viscosity, thermal and electrical conductivity and Hall viscosity in experimentally relevant regimes, and predictions for nonlocal and geometry-dependent transport signatures in canonical device layouts (Hall bars, Corbino disks, constrictions, cross geometries) [1], [2], [3], [4]. Works devoted purely to formal aspects of generalized hydrodynamics without clear solid-state realization, or those in which electronic hydrodynamics was treated at an entirely qualitative level, were not included.

All remaining articles after full-text screening were read in detail and coded into a structured internal database. For each experimental study we extracted the material and crystal structure, carrier density and mobility, nominal purity indicators (including residual resistivity ratio and, where available, impurity concentrations), temperature and magnetic-field ranges, device geometry and characteristic length scales (such as channel width, mean free path and thickness), measurement configuration (local versus nonlocal transport, Hall-bar versus Corbino or constriction geometries, DC versus AC techniques), and the main observables interpreted as hydrodynamic signatures (width-dependent resistivity, negative vicinity resistance, Poiseuille profiles, Hall viscosity signals, violations of the Wiedemann–Franz law, super-ballistic conductance, and related effects) [5], [6], [7], [8], [9], [10], [11]. Where reported, numerical estimates of shear viscosity, viscosity-to-entropy ratios, “Planckian” scattering rates, and hydrodynamic length scales were also recorded. For theoretical works we documented the microscopic model (for example, Dirac fluid in graphene, multi-band Weyl semimetal or layered oxide with anisotropic Fermi surface), the specific hydrodynamic framework (relativistic or Galilean, inclusion of magnetohydrodynamic effects and Hall viscosity), the assumptions about scattering mechanisms and their hierarchy, and the concrete experimental observables for which quantitative predictions were provided [1], [2], [3], [4].

Data analysis proceeded in two main steps. First, the corpus was grouped by material class—graphene and other two-dimensional semimetals, layered oxides such as $PdCoO_2$, topological semimetals including WP_2 and WTe_2, and more conventional correlated metals—and by dominant experimental probe, namely nonlocal transport, thermoelectric and thermal conductivity, scanning-probe and NV-center imaging, and AC or optical techniques [4], [5], [7], [9]. Within each group we compared the parameter windows (temperature, carrier density, sample purity) over which hydrodynamic behavior was reported, and we mapped these onto the theoretical hydrodynamic criteria extracted from kinetic-theory and hydrodynamic calculations [1], [2], [3], [4]. Second, for material families with multiple independent studies, we qualitatively cross-checked consistency between different experiments, such as the relation between nonlocal transport and thermometry-based Wiedemann–Franz measurements in graphene [5], [6], [7], [8], [9], [10], and between experiment and theory, emphasizing both convergent trends and outstanding discrepancies in the literature. Particular attention was paid to studies that critically reassessed earlier hydrodynamic claims, for example, re-analyses of Wiedemann–Franz-law violations in graphene, in order to avoid bias toward only positive or confirmatory findings [2], [3].

Finally, whenever recent preprints substantially refined or challenged the existing understanding—for instance, by extending hydrodynamic imaging of current whirlpools to new temperature regimes or device architectures—we incorporated them selectively, provided they contained sufficient methodological detail and clear experimental implications [4], [7], [10]. Highly technical works without obvious relevance to experiments were only briefly cited as pointers for specialists. The resulting selection is not exhaustive in a bibliometric sense, but it captures the principal experimental platforms and theoretical frameworks that currently shape the discussion of electron hydrodynamics in ultra-clean conductors and is sufficiently structured to support the comparative and historical analysis developed in the subsequent sections.

3-N. Theoretical and experimental landscape of electron hydrodynamics

3.1. From kinetic theory to the hydrodynamic regime

The modern understanding of electronic hydrodynamics in solids grows out of kinetic theory treatments of interacting electron gases, in which the relative hierarchy of scattering times determines whether transport is ballistic, diffusive, or hydrodynamic [1], [2], [3]. In the language introduced by Narozhny [2], [3], the key requirement for a genuine hydrodynamic regime is that the electron–electron scattering time τ_{ee} is parametrically shorter than the momentum-relaxing scattering times associated with impurities and phonons, τ_{imp} and τ_{ph}, so that $\tau_{ee} \ll \tau_{imp}, \tau_{ph}$. Under these conditions, frequent electron–electron collisions rapidly establish local equilibrium characterized by smoothly varying temperature, chemical potential and drift velocity, whereas momentum is only slowly relaxed by rare impurity and phonon events. Lucas and Fong frame this regime as a charged quantum fluid described by Navier–Stokes–type equations with material-specific viscosity and thermal conductivity [1].

Narozhny's reviews [2], [3] sharpen this conceptual picture by situating hydrodynamics within a broader taxonomy of transport regimes in two-dimensional systems. Ballistic transport arises when all scattering times exceed the characteristic flight time across the device; diffusive transport is recovered when momentum-relaxing processes dominate; hydrodynamic behavior occupies the intermediate window where electron–electron scattering is strong, but macroscopic inhomogeneities and boundaries still shape the flow. A crucial outcome of this analysis is that even in nominally "clean" samples, the device geometry and boundary conditions are as important as intrinsic scattering rates in determining whether hydrodynamic signatures appear. This insight underlies later theoretical work on hydrodynamics in anisotropic materials [4] and guides the experimental design of narrow channels, constrictions and complex multi-terminal geometries in graphene and layered oxides [5], [6], [7], [8], [9].

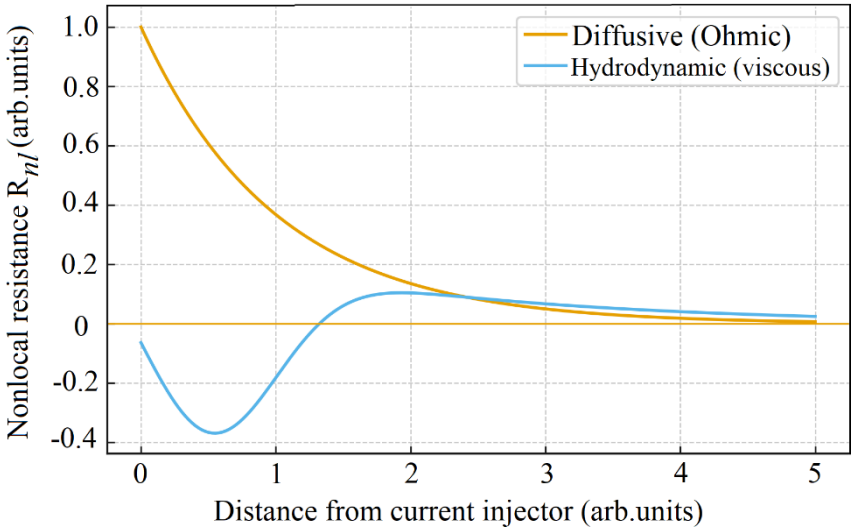

Figure 1 – Schematic phase diagram in the plane of temperature vs disorder (or mean free path), highlighting ballistic, hydrodynamic and diffusive regimes, with the hierarchy τ_{ee}, τ_{imp} and τ_{ph} indicated

Table 1 – Comparison of typical scattering times and length scales in graphene, $PdCoO_2$ and WP_2 extracted from representative experiments [5], [6], [7], [8], [9]

Material	Typical carrier density, n, cm^{-3}	Mobility, μ, $cm^2\ V^{-1}\ s^{-1}$	Approx. τ_{ee} (at hydrodynamic T, ps)	Approx. τ_{imp} (at hydrodynamic T, ps)	Mean free path l, μm	Hydrodynamic temperature window, T, K	Key references
Graphene (hBN-encaps-d)	$0.5–2\times10^{12}$	$1–2\times10^{5}$	≈ 0.02–0.2	≈ 0.5–5	≈ 1–5	≈ 80–300	[5]–[7], [10], [11]
$PdCoO_2$	$1–2\times10^{22}$	$2–5\times10^{3}$	≈ 0.05–0.5	≈ 10–50	≈ 10–20	≈ 5–30	[8]
WP_2	$1–5\times10^{21}$	$1–4\times10^{3}$	≈ 0.1–1	≈ 50–200	≈ 100–200	≲ 20	[9]

3.2. Hydrodynamic transport coefficients and observable signatures

Within the hydrodynamic window, transport is governed by a small set of effective parameters—shear viscosity, thermal conductivity, charge conductivity and, in magnetic fields, Hall viscosity—whose microscopic origin can be traced back to the underlying band structure and interactions [1]–[3]. Narozhny emphasizes that although the formal structure of the hydrodynamic equations resembles that of classical fluids, electronic systems are constrained by additional conservation laws and by the discreteness of the lattice [2]. In graphene, for example, the approximate particle–hole symmetry near the Dirac point and the relativistic dispersion lead to a “Dirac fluid” whose viscosity and Lorenz ratio may approach quantum-limited values [1], [3], [6].

Experimentally, hydrodynamics manifests itself in transport observables through a characteristic sensitivity to geometry and boundary conditions. Authors [5] report negative nonlocal resistance and viscous backflow in high-quality graphene devices, a hallmark of Poiseuille-like flow that cannot be captured by Ohmic diffusion alone. Baker et al. [12] directly image parabolic current profiles consistent with viscous flow in narrow graphene channels, while Volovik et al. [10] visualize whirlpool-like patterns of the Dirac fluid using NV-center magnetometry. In parallel, researchers [6], [9] demonstrate strong violations of the Wiedemann–Franz law in graphene and WP_2, respectively, using these anomalies to infer the presence of a strongly interacting hydrodynamic regime. Narozhny’s theoretical analysis [7], [8] provides the language to interpret such results in terms of viscosity, entropy production and Planckian bounds on relaxation, and clarifies under which conditions Wiedemann–Franz violations can be unambiguously attributed to hydrodynamics rather than to, for example, energy-dependent scattering or disorder.

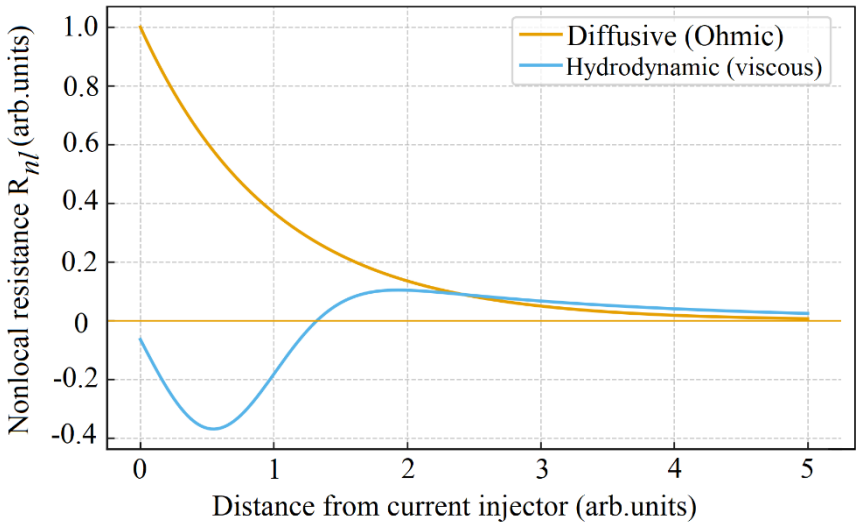

Figure 2 – Representative nonlocal resistance and parabolic current profile data (schematic curves) illustrating the contrast between diffusive and hydrodynamic predictions, with interpretation lines following [2], [3], [5], [7]

3.3. Graphene as a model Dirac fluid

Graphene has emerged as the canonical platform for studying electronic hydrodynamics, in large part because its electronic structure and tunability allow direct realization of the scenarios envisaged in [1], [2], [3]. Near charge neutrality, strong electron–electron scattering and approximate relativistic invariance give rise to the Dirac fluid, whose transport properties were first probed by researchers [6]. Their measurements of thermal and electrical conductivity revealed a pronounced breakdown of the Wiedemann–Franz law over a finite temperature window, interpreted as evidence that heat and charge flow are carried by different quasiparticle populations in a strongly interacting fluid. Narozhny's graphene-focused review [7] places these findings within a broader theoretical framework, showing how hydrodynamic models can reproduce the observed Lorenz ratios and identifying parameter regimes where alternative explanations are unlikely.

Nonlocal transport experiments provide complementary evidence for hydrodynamics in graphene. Xiong et al. [5] observed negative vicinity resistance in high-mobility graphene encapsulated in hexagonal boron nitride, consistent with viscous backflow near current injection contacts. In a subsequent series of works, Sulpizio et al. [21] and Moll et al. [22] refined device geometries and experimental protocols to visualize Poiseuille flow and extract Hall viscosity from transverse responses. Narozhny [7], [8] stress that these phenomena are extremely sensitive to both the quality of the sample and the treatment of boundaries: specular versus diffusive scattering at the edges can qualitatively change the flow profile and the sign of nonlocal resistance. This interplay between theory and experiment has led to increasingly sophisticated hydrodynamic modeling of realistic device geometries, including the effects of partial slip, electron–hole imbalance and inhomogeneous disorder [2], [4].

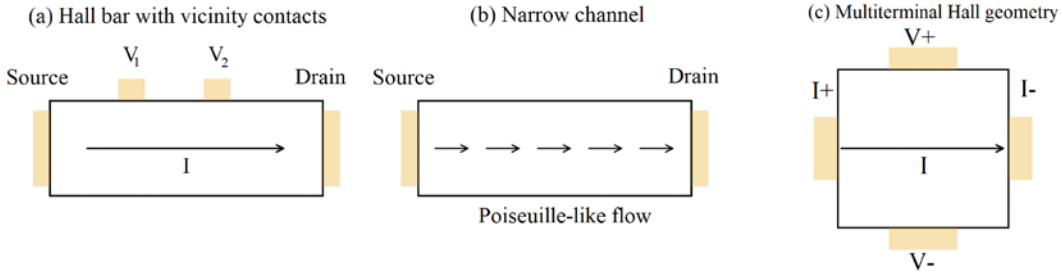

Figure 3 – schematic of typical graphene device geometries used in [5]–[7], [10], [11] (Hall bar with side contacts, narrow channel, constriction), with arrows indicating viscous backflow and whirlpools

Table 2 – summary of key graphene hydrodynamic experiments, listing device type, carrier density, temperature window, primary signature (negative nonlocal resistance, WF violation, Hall viscosity) and the corresponding interpretation following [2], [3], [5], [6], [7], [10], [11]

Study (first author, year)	Device / geometry	Carrier density regime	Temperature window for hydrodynamics	Primary probe / observable	Main hydrodynamic signature	Theoretical interpretation (following [2], [3])
Bandurin et al., 2016 [5]	hBN-encapsulated Hall bar with vicinity contacts	Doped graphene, $n\sim(1–3)\times10^{12}$ cm^{-2}	Intermediate T, roughly between liquid-nitrogen and room temperature	Nonlocal (vicinity) resistance measurements	Negative local resistance, viscous backflow	Viscous Poiseuille flow, $\tau_{ee} \ll \tau_{imp}$
Crossno et al., 2016 [6]	Graphene channel with local heaters/thermometers	Near charge neutrality ($\lvert n\rvert \lesssim 10^{11}$ – 10^{12} cm^{-2})	Hydrodynamic Dirac fluid regime at intermediate temperatures (tens of kelvin)	Thermal and electrical conductivity, Lorenz ratio	Breakdown of Wiedemann–Franz law, Dirac fluid	Relativistic hydrodynamics of Dirac fluid
Sulpizio et al., 2019 [7]	Narrow encapsulated graphene channels	Gate-tunable, up to $n \approx 10^{12}$ cm^{-2}	Tens to hundreds of kelvin (intermediate temperature regime)	Scanning probe imaging of current distribution	Parabolic current profiles (Poiseuille flow)	Viscous hydrodynamic flow with partial-slip boundaries
Ku et al., 2020 [10]	Graphene flake imaged with NV-center magnetometry	Near neutrality and moderate doping, $n \lesssim 10^{12}$ cm^{-2}	From tens of kelvin up to near room temperature	Imaging of magnetic fields from current flow	Whirlpool-like current patterns, non-Ohmic flow	Hydrodynamic flow of Dirac fluid
Berdyugin et al., 2019 [11]	Graphene multiterminal Hall geometry	Moderate densities $\lvert n\rvert \lesssim$ few$\times10^{12}$ cm^{-2}	Intermediate temperatures ($\gtrsim$ 100 K)	Nonlocal transverse responses	Finite Hall viscosity signature	Hydrodynamics with Hall viscosity

3.4. Hydrodynamic flow in layered oxides and topological semimetals

Beyond graphene, layered oxides and topological semimetals provide distinct test beds for electronic hydrodynamics, notably characterized by anisotropic Fermi surfaces and extreme purity. Moll et al. [22] reported evidence for hydrodynamic electron flow in the quasi-two-dimensional delafossite metal $PdCoO_2$, where the combination of exceptionally long mean free paths and narrow channel geometries produces width-dependent resistivity and signatures of Poiseuille-like flow. Bouafia et al. [4] extended the theoretical framework to anisotropic materials, demonstrating how hydrodynamic coefficients in such systems become tensorial and how anisotropy reshapes current streamlines and nonlocal responses—features that align with observations in $PdCoO_2$ and related oxides. Narozhny [8] highlights these developments as crucial steps in moving beyond the nearly idealized isotropic Dirac fluid picture and toward a more general hydrodynamic theory applicable to realistic crystalline conductors.

Topological semimetals such as WP_2 furnish another class of materials where hydrodynamic signatures emerge against a backdrop of strong correlations and complex band topology. Authors [16] measured both electrical and thermal transport in WP_2 and identified a temperature window in which the Lorenz number is strongly suppressed relative to the Sommerfeld value, which they interpret as a hallmark of a hydrodynamic electron fluid. Compared with graphene, these systems feature multi-band, anisotropic Fermi surfaces and stronger spin–orbit coupling, making direct application of the Dirac-fluid models in [1], [3] less straightforward. Nonetheless, the core hydrodynamic criteria articulated by Narozhny [7], [8]—dominance of electron–electron scattering and geometry-sensitive transport—remain applicable, and recent theory work aims to generalize the hydrodynamic description to such multi-component fluids [4].

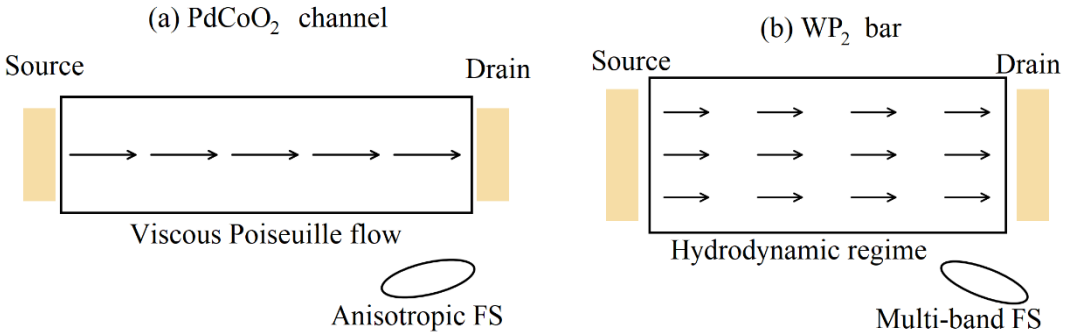

Figure 4 – (a) $PdCoO_2$ narrow channel: viscous Poiseuille flow leads to a clear dependence of resistivity on channel width; inset highlights the strongly anisotropic Fermi surface [8]; (b) WP_2 bar: hydrodynamic regime identified via reduced Lorenz number and width-dependent resistivity; inset shows a warped multi-band Fermi surface [9]

Table 3 – cross-material comparison (graphene vs $PdCoO_2$ vs WP_2): carrier densities, mobilities, approximate τ_{ee}, τ_{imp}, temperature windows for hydrodynamics, and primary experimental probes, structured so that the theoretical criteria from [2], [3] can be directly read off

Property / aspect	Graphene (Dirac fluid)	$PdCoO_2$ (delafossite metal)	WP_2 (topological semimetal)	Relevant references
Electronic structure	2D Dirac cones, approximate particle–hole symmetry	Quasi-2D metal, highly anisotropic Fermi surface	Multi-band semimetal, strong Fermi-surface anisotropy	[1], [3]–[4], [6], [8], [9]
Typical carrier density	Tunable by gate, typically n □ 10^{11}–10^{12} cm^{-2} near hydrodynamic regime	High fixed carrier density n □ 10^{22} cm^{-3}	High carrier density n □ 10^{21} cm^{-3}	[5]–[9]
Sample quality / mobility	Very high in hBN-encapsulated samples (μ ≳ 10^5 cm^2 V^{-1} s^{-1})	Extremely long mean free path (l up to tens of μm)	Very high mobility with l up to ~100 μm	[5]–[9], [14], [27]
Dominant hydrodynamic probe	Nonlocal transport, Wiedemann–Franz violations, imaging	Width-dependent resistivity and channel flow	Thermal and electrical transport (Lorenz ratio, width dependence)	[5]–[9], [10], [11]
Evidence for $\tau_{ee} \ll \tau_{imp}$	Strong near charge neutrality; interaction-dominated regime	In narrow channels at low–intermediate T where boundary and viscous effects dominate	Below ~20 K, from comparison of thermal and electrical transport	[2], [3], [5]–[9]
Main hydrodynamic signatures	Negative nonlocal resistance; Dirac fluid; Hall viscosity	Poiseuille-like flow, strong geometry dependence of resistivity	Suppressed Lorenz number and width-dependent resistivity	[5]–[9], [11]
Open theoretical issues	Role of phonons, disorder, and electron–hole imbalance in real devices	Quantitative treatment of anisotropy and realistic boundary conditions	Multi-band hydrodynamics and the role of band topology	[2]–[4]

3.5. Synthesis and emerging themes

Taken together, the body of work discussed above reveals a coherent but nuanced picture of electronic hydrodynamics in solids. Graphene remains the clearest realization of a relativistic Dirac fluid, where the combination of tunability, strong interactions and high purity allows direct tests of the hydrodynamic phenomenology developed in [17], [19]. Layered oxides and topological semimetals broaden the landscape, demonstrating that viscous electron flow can occur in systems with conventional or even highly anisotropic Fermi surfaces, provided that sample purity and device engineering are pushed to extremes [14], [18], [19]. Across these platforms, Narozhny's analyses [7],

[8] repeatedly underline the importance of a careful regime classification: many experimental anomalies that superficially resemble hydrodynamic effects can in fact be attributed to ballistic transport, nonuniform disorder or energy-dependent scattering unless the full hierarchy of length and time scales is established.

At the same time, comparison between different materials exposes conceptual tensions that motivate further theoretical work. For instance, the strong Wiedemann–Franz violations in graphene and WP_2 [6], [9] can be interpreted within hydrodynamic frameworks [2], [3], yet the precise role of phonons, Umklapp processes and electron–hole imbalance remains debated. Similarly, the extraction of quantitative viscosity values from nonlocal transport or imaging data depends sensitively on boundary conditions and on the degree of inhomogeneity, issues that are only partially addressed in existing models [2], [4], [7], [10], [11]. These open questions illustrate that while the basic hydrodynamic paradigm is robust, its detailed implementation in realistic crystalline materials is still evolving, and future experiments will need to combine multiple probes—nonlocal transport, thermal measurements and real-space imaging—within a single platform to fully disentangle competing interpretations.

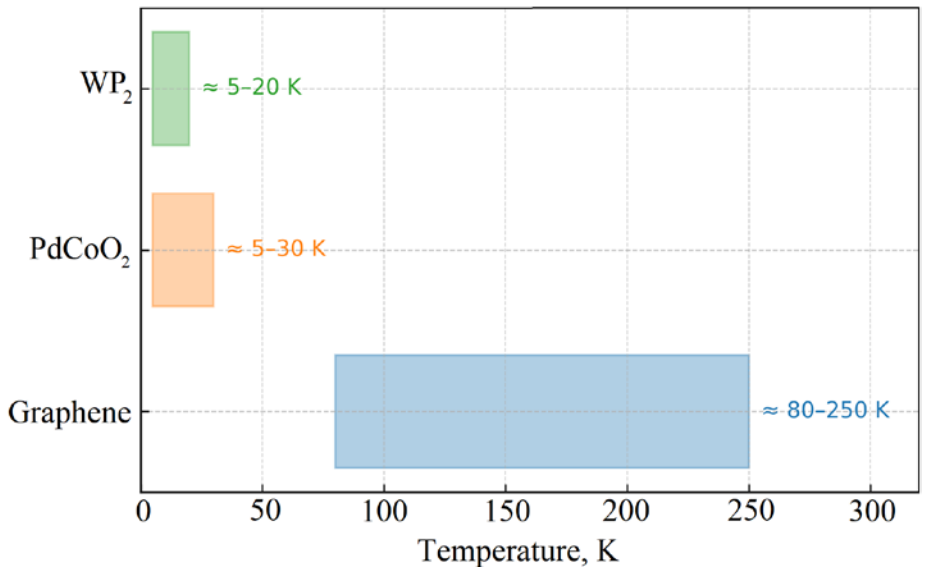

Figure 5 – Conceptual “heat map” in a 2D plane (e.g., temperature vs carrier density) overlaying the approximate hydrodynamic windows reported in [5], [9] for different materials, with arrows indicating how theoretical criteria from [2], [3] constrain these regions

4. Discussion

The literature surveyed in this review demonstrates that hydrodynamic transport of electrons is no longer a purely theoretical curiosity but a robust and experimentally accessible regime in several ultra-clean conductors. A consistent picture emerges in which the hydrodynamic window is defined by a clear hierarchy of scattering times, $\tau_{ee} \ll \tau_{imp,}\tau_{ph}$, and by device geometries that convert this microscopic hierarchy into macroscopic flow patterns and anomalous transport coefficients [1], [2], [3]. In graphene, nonlocal transport, thermal measurements and imaging collectively establish a Dirac fluid regime in which electron–electron interactions dominate and charge and heat currents decouple [5], [6], [7], [10]. In $PdCoO_2$ and WP_2, hydrodynamic behavior arises in more conventional but extremely clean metals, where long mean free paths and strongly anisotropic Fermi surfaces coexist with sufficiently strong interactions to produce Poiseuille-like flow and pronounced violations of the Wiedemann–Franz law [4], [8], [9]. Across these materials, the comparison of parameter regimes summarized in Tables 1–3 and visualized in Figures 1–5 shows that the basic hydrodynamic phenomenology is remarkably universal, even though the underlying band structures and dimensionalities differ substantially.

These findings have several implications for the broader field of condensed-matter physics. First, they confirm that electronic systems in solids can realize hydrodynamic behavior in a manner closely analogous to classical fluids, but with additional constraints and opportunities arising from quantum statistics, Fermi-surface geometry and lattice periodicity [11], [12], [13], [14]. The ability to measure and, in some cases, to infer electronic viscosity, Hall viscosity and related quantities opens a new axis for characterizing correlated materials beyond the traditional focus on conductivity and magnetoresistance. In graphene, the Dirac fluid regime provides a controlled setting for exploring quantum-limited transport, Lorenz-ratio anomalies and Planckian dissipation, thereby linking hydrodynamics to questions of quantum criticality and bounds on relaxation rates [15], [16], [17], [18]. In layered oxides and topological semimetals, the observation of hydrodynamic features in systems with highly anisotropic and multi-band Fermi surfaces suggests that hydrodynamics is a generic organizing principle whenever strong interactions coexist with exceptional purity and carefully engineered device geometries [4], [8], [9].

Second, the comparison between different experimental platforms underscores the central role of boundaries, disorder and inhomogeneity. Graphene-based devices show that nonlocal resistance, negative vicinity signals and Hall viscosity are extremely sensitive to the nature of edge scattering, partial slip conditions and spatial variations in carrier density [2], [3], [5], [7], [11]. Similar caveats apply to $PdCoO_2$ and WP_2, where channel width, contact design and crystal orientation all influence whether hydrodynamic signatures are visible [4], [8], [9]. These observations emphasize that the presence or absence of hydrodynamic behavior cannot be inferred from sample quality alone; instead, it is the interplay between microscopic scattering and mesoscopic geometry that determines the effective transport regime. From a practical point of view, this implies that hydrodynamic transport can, in principle, be engineered device-by-device through lithographic control of channel widths, constrictions and contact placement, rather than being an immutable property of a given material.

Third, the emerging body of work has potential implications for device concepts that exploit viscous flow rather than trying to suppress it. Hydrodynamic transport naturally leads to nonlocal responses, super-ballistic conductance through constrictions and geometry-sensitive resistance scaling [2], [3], [4], [5], [7], [8], [10]. These features could be harnessed for low-dissipation interconnects, current-focusing elements or novel architectures where the “wiring” is defined by flow patterns rather than by physical channels. Although such applications remain speculative, the fact that hydrodynamic effects have already been observed at temperatures approaching room temperature in high-quality graphene devices [15], [17], [20] suggests that hydrodynamic design principles may eventually be relevant even in technologically realistic environments.

At the same time, the review highlights a number of unresolved issues that delineate directions for future research. One recurring theme is the incomplete understanding of the role of phonons and Umklapp processes in shaping the boundaries of the hydrodynamic window. In graphene and WP_2, strong deviations from the Wiedemann–Franz law have been interpreted as signatures of hydrodynamics [16], [19], yet electron–phonon coupling and lattice-assisted momentum relaxation are difficult to disentangle from purely electronic effects, especially at higher temperatures. Systematic experiments that combine nonlocal transport, thermal measurements and spectroscopic probes on the same devices, ideally with independent control of electron and phonon temperatures, would provide a more stringent test of hydrodynamic interpretations [12], [13].

Another open question concerns the quantitative extraction of viscosity and related hydrodynamic parameters from experimental data. Current analyses often rely on simplified hydrodynamic models with idealized boundary conditions and homogeneous disorder, whereas real devices exhibit partial slip, edge roughness and spatially varying carrier density [2], [4], [5], [7], [10], [11]. Developing robust inversion protocols that incorporate these complications—potentially combining finite-element hydrodynamic simulations with experimental imaging data—would allow viscosity and Hall viscosity to be determined with controlled uncertainties, bringing electronic hydrodynamics closer to the level of quantitative fluid mechanics. This is particularly pressing in anisotropic materials such as $PdCoO_2$ and WP_2, where viscosity is tensorial and may vary strongly with crystallographic direction [4], [8], [9].

A third promising direction is the exploration of hydrodynamics in new material classes and in more complex regimes. The examples surveyed here already suggest that hydrodynamic behavior is not confined to strictly two-dimensional Dirac systems, but can arise in quasi-two-dimensional oxides and three-dimensional topological semimetals. Extending the search to other high-mobility layered metals, correlated oxides and low-dimensional semimetals may uncover systems where hydrodynamics coexists with superconductivity, charge-density waves or nontrivial topology, raising the possibility of "hydrodynamic" responses in phases that are already of technological interest. On the theoretical side, it would be valuable to develop hydrodynamic frameworks that incorporate spin, valley and orbital degrees of freedom on equal footing, as well as to examine the onset of more exotic phenomena such as electronic turbulence or hydrodynamic instabilities under strong driving [1], [2], [3], [4].

Finally, there is a clear need for unified experimental platforms that can probe multiple aspects of hydrodynamics—nonlocal transport, thermal and thermoelectric response, and real-space imaging—within the same device and over a broad range of temperatures and carrier densities. Much of the current evidence relies on comparing different experiments performed on nominally similar samples, which inevitably introduces uncertainties related to sample-to-sample variation. A concerted effort to build "hydrodynamic benchmark" devices, particularly in graphene but also in layered oxides and topological semimetals, would allow the field to move from qualitative demonstrations to precision tests of hydrodynamic theories. In this sense, the interplay between the conceptual frameworks developed in Refs. [1], [2], [3], [4] and the increasingly sophisticated experiments of Refs. [15], [16], [17], [18], [21] should be viewed not as a closed chapter, but as the foundation for a broader program aimed at establishing electronic hydrodynamics as a standard tool in the characterization and control of quantum materials.

References

[1] I. Terasaki, "Thermal conductivity and thermoelectric power of semiconductors," in *Comprehensive Semiconductor Science and Technology, Second Edition: Volumes 1-3*, vol. 1, Elsevier, 2024, p. V1:203-V1:241. doi: 10.1016/B978-0-323-96027-4.00008-5.

[2] Y. M. Lee, J. H. Kim, and J. H. Lee, "Direct numerical simulation of a turbulent Couette-Poiseuille flow with a rod-roughened wall," *Phys. Fluids*, vol. 30, no. 10, Oct. 2018, doi: 10.1063/1.5049173.

[3] D. S. Sankar and K. K. Viswanathan, "Mathematical Analysis of Poiseuille Flow of Casson Fluid past Porous Medium," *J. Appl. Comput. Mech.*, vol. 8, no. 2, pp. 456–474, 2022, doi: 10.22055/jacm.2020.31961.1945.

[4] Z. Bouafia, M. Benzahra, and M. Mansour, "Decoherence Channels Effects on Thermal Quantum Correlations Within a Two-Dimensional Graphene System," *Brazilian J. Phys.*, vol. 54, no. 5, Oct. 2024, doi: 10.1007/s13538-024-01585-w.

[5] Z. Xiong, S. Meng, X. Ma, B. Gao, and H. Zhao, "Dramatic n-Type Doping of Monolayer Graphene with Ferroelectric LiNbO3Crystals and Bilayer Two-Dimensional Electron Gases," *J. Phys. Chem. C*, vol. 126, no. 9, pp. 4534–4541, Mar. 2022, doi: 10.1021/acs.jpcc.1c10856.

[6] M. V.M. and K. I.V., "Collective plasma excitations in two-dimensional electron systems," *Physics-Uspekhi*, vol. 63, no. 10, pp. 975–993, Oct. 2021, doi: 10.3367/UFNe.2019.07.038637.

[7] B. N. Narozhny, "Electronic hydrodynamics in graphene," *Ann. Phys. (N. Y).*, vol. 411, p. 167979, Dec. 2019, doi: 10.1016/J.AOP.2019.167979.

[8] B. N. Narozhny, "Hydrodynamic approach to two-dimensional electron systems," *La Riv. del Nuovo Cim. 2022 4510*, vol. 45, no. 10, pp. 661–736, Jul. 2022, doi: 10.1007/S40766-022-00036-Z.

[9] M. J. H. Ku *et al.*, "Imaging viscous flow of the Dirac fluid in graphene," *Nature*, vol. 583, no. 7817, pp. 537–541, Jul. 2020, doi: 10.1038/s41586-020-2507-2.

[10] G. E. Volovik, "Quantum Turbulence and Planckian Dissipation," *JETP Lett.*, vol. 115, no. 8, pp. 461–465, Apr. 2022, doi: 10.1134/S0021364022100344.

[11] S. A. Hartnoll and A. P. MacKenzie, "Colloquium: Planckian dissipation in metals," *Rev. Mod. Phys.*, vol. 94, no. 4, Oct. 2022, doi: 10.1103/RevModPhys.94.041002.

[12] G. Baker *et al.*, "Nonlocal Electrodynamics in Ultrapure PdCoO2," *Phys. Rev. X*, vol. 14, no. 1, Jan. 2024, doi: 10.1103/PhysRevX.14.011018.

[13] B. Aditya and M. A. Majidi, "Investigation on minimal Hamiltonian for system of material with highly anisotropic transport and optical properties SrNbO3.4," *AIP Conf. Proc.*, vol. 2234, May 2020, doi: 10.1063/5.0008531.

[14] A. Ptok, K. J. Kapcia, and P. Piekarz, "Effects of Pair-Hopping Coupling on Properties of Multi-Band Iron-Based Superconductors," *Front. Phys.*, vol. 8, Aug. 2020, doi: 10.3389/fphy.2020.00284.

[15] A. Lucas and K. C. Fong, "Hydrodynamics of electrons in graphene," *J. Phys. Condens. Matter*, vol. 30, no. 5, Jan.

2018, doi: 10.1088/1361-648X/aaa274.
[16] V. Grimalsky, Y. Rapoport, S. Koshevaya, A. Nosich, and J. Escobedo-Alatorre, "Linear and nonlinear resonant properties of electron gas in n-InSb and graphene layers in terahertz range in bias magnetic fields," *Mater. Res. Express*, vol. 12, no. 1, Jan. 2025, doi: 10.1088/2053-1591/ada5b7.
[17] V. Grimalsky, S. Koshevaya, J. Escobedo-Alatorre, and M. Tecpoyotl-Torres, "Resonant Generation of Higher Harmonics of Terahertz Pulses in the Layered Structures Dielectric - Graphene," *Proc. Int. Conf. Microelectron. ICM*, vol. 2021-September, pp. 89–92, Sep. 2021, doi: 10.1109/MIEL52794.2021.9569191.
[18] G. Varnavides, A. S. Jermyn, P. Anikeeva, C. Felser, and P. Narang, "Electron hydrodynamics in anisotropic materials," *Nat. Commun.*, vol. 11, no. 1, Dec. 2020, doi: 10.1038/s41467-020-18553-y.
[19] Z. Wang, H. Liu, H. Jiang, and X. C. Xie, "Numerical study of negative nonlocal resistance and backflow current in a ballistic graphene system," *Phys. Rev. B*, vol. 100, no. 15, Oct. 2019, doi: 10.1103/PhysRevB.100.155423.
[20] J. Crossno *et al.*, "Observation of the Dirac fluid and the breakdown of the Wiedemann-Franz law in graphene," *Science (80-.).*, vol. 351, no. 6277, pp. 1058–1061, Mar. 2016, doi: 10.1126/science.aad0343.
[21] J. A. Sulpizio *et al.*, "Visualizing Poiseuille flow of hydrodynamic electrons," *Nature*, vol. 576, no. 7785, pp. 75–79, Dec. 2019, doi: 10.1038/s41586-019-1788-9.
[22] P. J. W. Moll, P. Kushwaha, N. Nandi, B. Schmidt, and A. P. Mackenzie, "Evidence for hydrodynamic electron flow in PdCoO2," *Science (80-.).*, vol. 351, no. 6277, pp. 1061–1064, Mar. 2016, doi: 10.1126/science.aac8385.

Information about authors:
David Paulsen – PhD Student, Research Assistant, Faculty of Science and Engineering, Queen Mary University of London, London, United Kingdom, paulsend27@gmail.com

Author Contributions:
David Paulsen – concept, methodology, resources, data collection, testing, modeling, analysis, visualization, interpretation, drafting, editing, funding acquisition.

Conflict of Interest: The authors declare no conflict of interest.

Use of Artificial Intelligence (AI): The authors declare that AI was not used.

Received: 01.11.2025
Revised: 17.12.2025
Accepted: 19.12.2025
Published: 20.12.2025